# Thomas mechanism in electron capture to the continuum

V. D. Rodríguez*

*Departamento de Física, Facultad de Ciencias Exactas y Naturales, Universidad de Buenos Aires, 1428 Buenos Aires, Argentina*

R. O. Barrachina*

*Comisión Nacional de Energía Atómica, Centro Atómico Bariloche e Instituto Balseiro, 8400 Bariloche, Argentina*

Thomas mechanism is theoretically shown to be present for the electron capture to the continuum (ECC) processes in ion-atom ionizing collisions. By focusing on the recoil-ion momentum distribution, a prominent peak structure at 60° from the backward direction is observed near the kinematical threshold. This recoil-ion critical angle corresponds to the Thomas double-scattering mechanism for electron capture. The theoretical description of this ECC Thomas peak in ionization collisions requires accounting for the interaction of the electron with both the projectile and the residual target.

PACS number(s): 34.50.Fa

## I. INTRODUCTION

Up to now, most of our understanding of single-ionization processes in ion-atom collisions has come from the study of singly and doubly differential cross sections of the projectile and/or the emitted electron. For instance, the electron velocity $\mathbf{v}_e$ distribution is known to show three conspicuous structures. These are a shoulder on a ''sphere'' centered on the projectile velocity $\mathbf{v}$ with a radius approximately equal to $v$, and two cusp-shaped peaks located at the origin and $\mathbf{v}$, respectively. The first of these structures is ascribed to a binary projectile-electron collision [1]. The peaks have been traditionally attributed to a mechanism where the ejected electron ends up in a low-lying continuum state of the ''charged'' residual target (''soft collision electrons'') [2] or the projectile [''electron capture to the continuum (ECC)''] [3–6].

A proper theoretical description of these peaks requires the analysis of the electron moving in the combined potential fields of the projectile and the residual target ion [7]. Thus, multiple scattering (i.e., three-body) effects could be important for understanding these features [8,9]. In the present paper we are interested in analyzing the role of double scattering effects in the electron capture to the continuum process.

Already in 1927, Thomas argued that the capture of an electron into a bound state of the projectile should be dominated at high impact energies by three-body effects [10]. Classically, for a heavy projectile $P$ to be able to capture an electron $e$ from an atom, a double-scattering mechanism would be necessary in order to lead the electron close to the projectile in velocity space. First, the electron has to be knocked by the projectile toward the target nucleus $T$ at an angle of 60° with a speed $\mathbf{v}_e \sim \mathbf{v}$. Then it has to undergo a second elastic collision with the target nucleus that deviates it back into the direction of the projectile. The momentum transfer to the electron in the first collision modifies the trajectory of the projectile by an angle $\theta_{\mathrm{Th}} \sim \sqrt{3} m_e/2M_P$, where $m_e$ and $M_P$ are the masses of the electron and the projectile,

respectively. In a quantum-mechanical description, this Thomas two-step process is reproduced by the second term in Born expansion [11,12]. At asymptotically high velocities, this term dominates over all other Born orders for electron capture [12]. In particular, exact numerical second Born calculations for 1s-1s charge exchange in $\mathrm{H}^+ + \mathrm{H}$ collisions have shown that a Thomas peak appears at this particular angle $\theta_{\mathrm{Th}}$ in the angular differential cross section for the scattering of the projectile at energies above 5 MeV [13]. Similar results were provided by continuum-distorted wave [14] and coupling-channel calculations [15]. Finally, the existence of this peak was experimentally verified in 1983 by Pedersen, Cocke, and Stöckli [16]. Dettmann [17] and Briggs [8] discussed the occurrence of a similar structure in the projectile's angular differential cross section for ECC, but argued that it should be negligible for ion scattering. We propose here a different approach to this subject and show in an unambiguous way the existence of the Thomas mechanism in ECC.

The advancement of experimental techniques, such as the cold-target recoil-ion momentum spectroscopy (COLTRIMS) [18–20], has provided a new tool for studying ion-atom ionization collisions by focusing not only on the projectile scattering and/or the electron emission, but also on the target-ion recoil [18]. One of the aspects of the enhanced picture provided by the analysis of the third collision partner is the relationship between the kinematical threshold of the longitudinal recoil-ion momentum $P_{R\parallel}$ and the ECC process [21,22]. Moreover, while the single differential cross section in the projectile's angle diverges for the ECC process, the recoil-ion momentum distribution remains finite at the kinematical threshold.

In this paper, we take advantage of this fact to look for a fingerprint of the Thomas mechanism in the ECC process. The theory is outlined in the next section, followed by the results section.

## II. THEORY

Generally, the double differential cross sections in the recoil-ion momentum $\mathbf{P}_R$ (DDCS) can be obtained from the

---

*Also a member of the Consejo Nacional de Investigaciones Científicas y Técnicas.

ionization transition matrix $T_{if}$ by (atomic units are used throughout) [22]

$$\frac{d\sigma}{d\mathbf{P}_R} = \frac{1}{4\pi^2 v^2} \int |T_{if}|^2 \, \delta(\mathbf{P}_{R\perp} - \mathbf{q} + \mathbf{v}_{e\perp})$$

$$\times \delta\left( P_{R\parallel} + \frac{v}{2} - \frac{|\varepsilon_i|}{v} - |\mathbf{v}_e - \mathbf{v}|^2/2v \right) d^3\mathbf{v}_e d^2\mathbf{q}, \quad (1)$$

where $\mathbf{q}$ is the perpendicular projectile transfer momentum and $\varepsilon_i$ is the initial binding energy of the target electron. $(P_{R\parallel})$ and $(P_{R\perp})$ are the components of the recoil-ion momentum parallel and perpendicular to the impact velocity, respectively. In this equation we have neglected terms of order $1/M_P$ and $1/M_T$, where $M_P$ and $M_T$ are the masses of the projectile and target, respectively. We clearly see that there exists a threshold in the longitudinal recoil-ion momentum given by

$$P_{R\parallel}^{min} = -\frac{v}{2} + \frac{|\varepsilon_i|}{v}, \quad (2)$$

which corresponds to $\mathbf{v}_e = \mathbf{v}$, this is to the ECC peak in the electron velocity distribution.

Owing to the delta functions in expression (1), we may readily obtain

$$\frac{d\sigma}{d\mathbf{P}_R} = \frac{v'}{4\pi^2 v} \int |T_{if}|^2 d\hat{\mathbf{v}}' \quad (3)$$

where the remaining integral is taken over the solid angle of the relative electron-projectile velocity $\mathbf{v}' = \mathbf{v}_e - \mathbf{v}$, the transverse momentum conservation should be considered in the $T$-matrix element calculation, and

$$v' = \sqrt{2v(P_{R\parallel} - P_{R\parallel}^{min})}. \quad (4)$$

According to the final-state interaction theory [23], the behavior of the ionization cross section for small values of the relative electron-projectile velocity (i.e., for $P_{R\parallel} \approx P_{R\parallel}^{min}$) can be shown to be dominated by the normalization of the corresponding continuum wave function $\Psi_{\mathbf{v}'}(\mathbf{r}')$ for the electron-projectile system [24], namely,

$$\frac{d\sigma}{d\mathbf{P}_R} = F(v') \frac{d\tilde{\sigma}}{d\mathbf{P}_R}, \quad (5)$$

with $F(v') = (2\pi)^3 |\Psi_{\mathbf{v}'}(0)|^2$. From Eqs. (3) and (5), the reduced DDCS $d\tilde{\sigma}/d\mathbf{P}_R$ goes linearly to zero as $v' \to 0$ near the threshold. However, in this limit the distortion factor $F(v')$ diverges as

$$F(v') \approx \frac{2\pi Z_P}{v'} \quad (6)$$

for an ionic projectile of charge $Z_P > 0$, and therefore $d\sigma/d\mathbf{P}_R$ is finite at threshold.
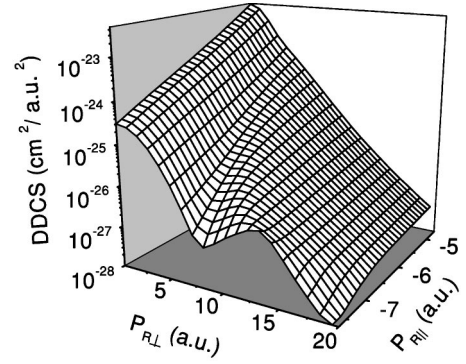


FIG. 1. CDW-EIS calculation of the recoil-ion doubly-differential momentum distribution for single ionization of Helium by 6 MeV proton impact as a function of the recoil-ion momentum components $P_{R\parallel}$ and $P_{R\perp}$ close the $P_{R\parallel}$ threshold.

We evaluate the recoil-ion momentum distribution $d\sigma/d\mathbf{P}_R$ near this threshold by means of the continuum distorted wave-eikonal initial state (CDW-EIS) approximation, as introduced by Crothers and McCann [25] for ion-atom ionizing collisions. While the initial scattering state is distorted by an eikonal phase factor for the electron-projectile Coulomb interaction, the final state incorporates the interaction of the emitted electron with both the projectile and the residual target ion through a product of the corresponding individual Coulomb continuum wave functions. The internuclear interaction is accounted for as explained in Ref. [26]. We employ an independent electron description of the two-electron target atom [7].

## III. RESULTS

We evaluate the recoil-ion DDCS for the ionization of helium by 6 MeV proton impact. The results are shown in Fig. 1 as a function of the recoil-ion momentum components $P_{R\perp}$ and $P_{R\parallel}$. A peak for $P_{R\perp} \sim 13.4$ a.u. at the kinematical threshold ($P_{R\parallel} \sim -7.7$ a.u.) can be clearly observed in Fig. 1. The recoil-ion momentum makes an angle $\chi_R = 90° + \tan^{-1}(P_{R\parallel}/P_{R\perp})$ measured from the backward direction. Thus the structure occurs at an angle from the backward direction equal to $\chi_R = \chi_{Th} \sim 60°$, exactly as expected for the recoil-ion in the Thomas process. In fact, in the second step of the Thomas mechanism the target nucleus is knocked by the electron with velocity $v$. After the collision, the electron has changed its direction by approximately $60°$ toward the forward direction, transferring to the target-ion a momentum $\mathbf{P}_R$ with module $v$ and whose direction forms an equilateral triangle with the initial and final electron velocities, namely $\chi_R \sim 60°$. It can be easily verified with the two values above that the structure in Fig. 1 appears at $P_R \sim 15.5$ a.u., i.e., the ion velocity for 6 MeV proton impact.

Since $P_{R\parallel} = P_{R\parallel}^{min} + v'^2/2v$, as $P_{R\parallel}$ shifts away from the threshold value $P_{R\parallel}^{min}$, the collision departs from the electron capture to the continuum condition [21,22] and the Thomas peak disappears smoothly, as shown in Fig. 1.
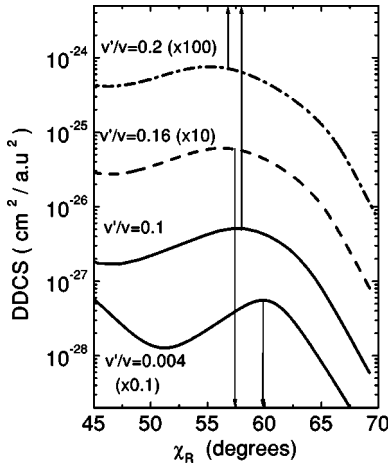
FIG. 2. Same as Fig. 1 but as a function of the recoil ion angle $\chi_R$ taken from the backward direction, for fixed values of $P_{R\parallel} = P_{R\parallel}^{min} + v'^2/2v$. The arrows mark the angle $\chi_R^-$, as defined in the text.

In Fig. 2 we show the recoil-ion DDCS near the threshold for different values of $P_{R\parallel}$, as a function of the recoil-ion scattering angle from the backward direction. To each of these curves corresponds two values of the recoil angle for which the electron velocity is parallel to **v**, namely,

$$\chi_R^{\pm} = 90° - \frac{1}{2} \cos^{-1}\left(\frac{1 \pm v'/v}{2}\right) \qquad (7)$$

with $v' = \sqrt{2v(P_{R\parallel} - P_{R\parallel}^{min})}$. We see that the position of $\chi_R^-$, as marked in is figure, is close to the maximum of the DDCS, while there is a slight shoulder at $\chi_R^+ > 60°$. These results indicate that the Thomas mechanism in ECC also holds for final electron velocities slightly different from **v**.

With the objective of clarifying how the structure at 60° near the threshold associates to the Thomas mechanism, we employ different theoretical models to evaluate the recoil-ion DDCS. For instance, a simplified Born approximation in which the electron in the final state is described by a plane wave (Born-PW: dotted line) is known to explain the binary shoulder fairly well, but not the ECC process. Thus the recoil-ion DDCS goes to zero as $v' = \sqrt{2v(P_{R\parallel} - P_{R\parallel}^{min})} \to 0$. Therefore, we display it in Fig. 3 slightly away from this limit ($v' = 0.055$ a.u.). We clearly see that the Born-PW approximation fails to show any Thomas structure. However, it is important to point out that this is due to the absence of a second interaction of the electron with the target, and not to the vanishing of the cross section at threshold. In fact, the Born approximation (Born: dotted-dashed line) also vanishes at threshold, even though it correctly accounts for the Thomas peak. The reason is that, in contrast to the Born-PW approximation, this theory includes the $T$-$e$ interaction to all orders in addition to a first-order $P$-$e$ interaction. Therefore the theory accomplishes the Thomas double mechanism. However, since it does not include any final-state $P$-$e$ interaction, the corresponding recoil-ion DDCS also goes to zero
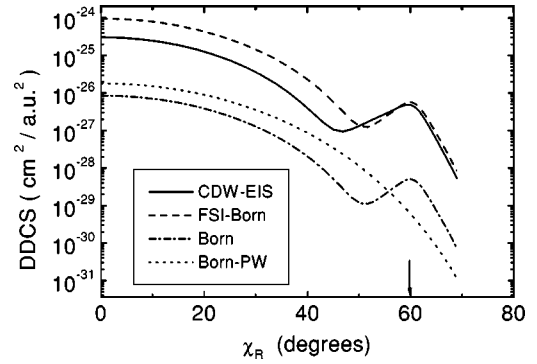


FIG. 3. Same as Fig. 2 with $v' = 0.055$ a.u. The Born plane-wave (dotted line), Born (dotted-dashed line) and final-state interaction Born (dashed line) approximations are also displayed.

at threshold as may be verified from Eq. (3). We multiply this DDCS by the distortion factor $F(v')$ that provides the ECC cusp in order to get the final-state interaction Born approximation (FSI-Born: dashed line). In spite of its simplicity, this theory is close to the refined CDW-EIS around the Thomas peak, since it accounts for the correct final-state dynamics at threshold. This simple model can be used to obtain a scaling rule with the projectile charge of the peak.

From the known $Z_P^2$ scaling of the Born approximation and the $Z_P$ behavior of the distortion factor $F(v')$, we predict the peak maximum to behave as $Z_P^3$. While the Thomas
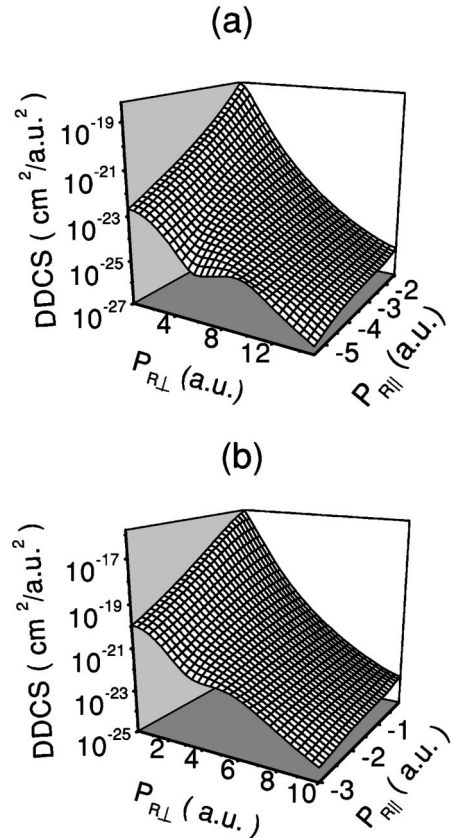


FIG. 4. Same as Fig. 1 but for (a) 3 MeV and (b) 1 MeV proton impact.

scattering angle for the projectile $\theta_{Th} \sim \sqrt{3} m_e / 2 M_P$ depends on the projectile mass, the corresponding one for the recoil ion $\chi_{Th}$ does not. Thus, while $\theta_{Th} \rightarrow 0$ as the projectile mass increases, which makes it hard to measure because of the tiny projectile deflection, $\chi_{Th}$ remains equal to 60° for any ionic specie. This represents one of the great advantages of using the recoil-ion for evidencing the Thomas double-scattering processes. In particular, the $Z_P^3$ scaling indicates that the Thomas structure in the recoil-ion DDCS would increase appreciably by using multiply charged projectiles.

We now study the behavior of the ECC Thomas peak when decreasing the impact energy. Figure 4 shows the recoil-ion momentum distribution for 3 MeV and 1 MeV proton impact energies. We observe how the peak structure becomes smoother as the impact energy decreases. This is due to the smearing of the structure by the initial momentum distribution of the electron in the target. Again, the structures are localized around $P_{R\parallel}$ and $P_{R\perp}$ complying with $\chi_R \sim 60°$ and $P_R = v$ for both cases.

## IV. FINAL REMARKS

In summary, we have shown how the recoil-ion momentum distribution may be used to identify the Thomas mechanism in electron capture to the continuum. The double scattering implied in the Thomas process is accounted for by the CDW-EIS approximation. The $Z_P^3$ scaling law of the cross sections around the Thomas peak may encourage experiments using the new COLTRIMS technique to verify experimentally our theoretical predictions.

[1] D.H. Lee, P. Richard, T.J.M. Zouros, J.M. Sanders, J.L. Shinpaugh, and H. Hidmi, Phys. Rev. A **41**, 4816 (1990).

[2] S. Suárez, C. Garibotti, W. Meckbach, and G. Bernardi, Phys. Rev. Lett. **70**, 418 (1993).

[3] G.B. Crooks and M.E. Rudd, Phys. Rev. Lett. **25**, 1599 (1970).

[4] A. Salin, J. Phys. B **2**, 631 (1969).

[5] J.H. Macek, Phys. Rev. A **1**, 235 (1970).

[6] L. Sarkadi, J. Pálinkás, A. Kóvér, D. Berényi, and T. Vajnai, Phys. Rev. Lett. **62**, 527 (1989).

[7] P.D. Fainstein, V.H. Ponce, and R.D. Rivarola, J. Phys. B **24**, 3091 (1991).

[8] J.S. Briggs, J. Phys. B **19**, 2703 (1986).

[9] S. Suárez, R.O. Barrachina, and W. Meckbach, Phys. Rev. Lett. **77**, 474 (1996).

[10] L.H. Thomas, Proc. R. Soc. London, Ser. B **114**, 561 (1927).

[11] R.M. Drisko, Ph.D. thesis, Carnegie Institute of Technology, 1955.

[12] R. Shakeshaft and L. Spruch, Rev. Mod. Phys. **51**, 369 (1979).

[13] P.R. Simony and J.H. McGuire, J. Phys. B **14**, L737 (1981); J.E. Miraglia, R.D. Piacentini, R.D. Rivarola, and A. Salin, *ibid.* **14**, L197 (1981).

[14] R.D. Rivarola, A. Salin, and M. Stockli, J. Phys. (France) Lett. **45**, L259 (1984); A.E. Martinez and R.D. Rivarola, J. Phys. B **23**, 4165 (1990).

[15] N. Toshima and J. Eichler, Phys. Rev. Lett. **66**, 1050 (1991).

[16] E. Horsdal-Pedersen, C.L. Cocke, and M. Stockli, Phys. Rev. Lett. **50**, 1910 (1983).

[17] K. Dettmann, K.G. Harrison, and M.W. Lucas, J. Phys. B **7**, 269 (1974).

[18] J. Ullrich, R. Moshammer, R. Dörner, O. Jagutzki, V. Mergel, H. Schmidt-Böcking, and L. Spielberger, J. Phys. B **30**, 2917 (1997).

[19] W. Schmitt, R. Moshammer, F.S.C. O'Rourke, H. Kollmus, L. Sarkadi, R. Mann, S. Hagmann, R.E. Olson, and J. Ullrich, Phys. Rev. Lett. **81**, 4337 (1998).

[20] Kh. Khayyat *et al.*, J. Phys. B **32**, L73 (1999).

[21] V.D. Rodríguez, Y.D. Wang, and C.D. Lin, Phys. Rev. A **52**, R9 (1995).

[22] V.D. Rodríguez and R.O. Barrachina, Phys. Rev. A **53**, 3335 (1996).

[23] J.R. Taylor, *Scattering Theory* (Wiley, New York, 1972).

[24] R.O. Barrachina, J. Phys. B **23**, 2321 (1990); R.O. Barrachina, Nucl. Instrum. Methods Phys. Res. B **124**, 198 (1997).

[25] D.S.F. Crothers and J.F. McCann, J. Phys. B **24**, 3091 (1983).

[26] V.D. Rodríguez, J. Phys. B **29**, 275 (1996).